75th International Astronautical Congress (IAC), Milan, Italy, 14-18 October 2024.

IAC-24-B2.IP.17.x80835

Verification of laser communication terminals for CubeSats as preparation for missions PIXL-1 and QUBE under atmospheric conditions

Benjamin Rödiger[a]*, René Rüddenklau[a], Anil Morab Vishwanath[a,b], Christian Roubal[a], Florian Moll[a], Christian Fuchs[a]

[a] *German Aerospace Center (DLR), Institute of Communications and Navigation, Muenchener Straße 20, 82234 Wessling, benjamin.roediger@dlr.de*
[b] *Airbus Defence and Space, Willy-Messerschmitt-Straße 1, 82024 Taufkirchen*
* Corresponding Author

Abstract

Laser communication enables high-rate and secure communication even on smallest satellites like CubeSats. The German Aerospace Center (DLR) demonstrated the capabilities and advantages of free-space optical communication in the PIXL-1 mission, with the first OSIRIS4CubeSat payload in space. As OSIRIS4CubeSat is a pure transmitter for classical optical communication, OSIRIS4QUBE marks the first evolution towards quantum key distribution (QKD). The goal in the QUBE project is to transmit, in addition to the classical optical signal, experimental QKD signals from a 3U CubeSat to the Optical Ground Station Oberpfaffenhofen. The QUBE mission foresees that Ludwig-Maximilian University of Munich and Max Planck Institute for the Science of Light provide experimental QKD signals from their in house developed payloads which are coupled into OSIRIS4QUBE using a fiber network. To prepare the laser communication terminals for the operation in space and to verify their functionalities, DLR tests its terminals during ground test campaigns. Therefore, a tracking and communication test over a 3 km free space track is performed which includes the final infrastructure at the receiver side and replicates the conditions of the final mission. Each test includes the engineering qualification model of the payload and one of DLR's optical ground stations. The optical ground stations are equipped with the optical uplink beacon system which is also being used during the operational missions. Engineering qualification and flight model of each terminal are identical to ensure that the measured acquisition and tracking behavior represents the final behavior. The free space channel over the test track includes atmospheric effects, which can hardly be replicated in a laboratory. All laser signals are optically attenuated to the respective power, which represents the distances between target and the satellite during the final mission. This ensures signal integrity as all systems can operate at nominal power. A hexapod on the transmitter side is used to reconstruct the trajectory of the satellite according to the expected movements. This paper describes the setup on the transmitter and the receiver side for both campaigns OSIRIS4CubeSat and OSIRIS4QUBE. The goal of the campaigns is to verify the acquisition and tracking behavior under realistic conditions and ensuring reliable data reception at the optical ground station. It discusses the calculated attenuations and the assumptions. The results of both ground test campaigns are shown, which proves that both terminals can fulfill their functionalities in space.

Keywords: Laser Communication, CubeSats, New Space, Quantum Key Distribution, OSIRIS

Acronyms/Abbreviations

4-quadrant diode (4-QD)
Attitude control system (ACS)
Coarse pointing assembly (CPA)
Digital analogue converter (DAC)
German Aerospace Center (DLR)
Erbium doped fiber amplifier (EDFA)
Engineering qualification model (EQM)
Friedrich-Alexander University (FAU)
Field of regard (FoR)
Fine pointing assembly (FPA)
Fine steering mirror (FSM)
Laser communication terminal (LCT)
Ludwig Maximilian University (LMU)
Max Planck institute for the science of light (MPL)
Neutral density (ND)
OSIRIS4CubeSat (O4C)
OSIRIS4QUBE (O4Q)
Optical ground station (OGS)
Optical space infrared downlink system (OSIRIS)
Pointing acquisition and tracking (PAT)
Reception (Rx)
Quantum key distribution (QKD)
Size Weight and Power (SWaP)
Transportable optical ground station (TOGS)
Transmission (Tx)

1. Introduction

Satellite communications are crucial for Earth observation missions to download the generated payload data to ground. It also increases in importance for global telecommunication systems, e.g. when mega-constellations are used for space network implementation. In both cases, the use of optical link

technology is a good choice to fulfil requirements on data throughput and hardware size, weight and power (SWaP) [1]. The SWaP requirements are especially important for CubeSat platforms. Optical link technology is also the basis for quantum communication between space and Earth. With this, satellite quantum key distribution (QKD) systems can be realized that enable delivery of quantum secure keys on a global level [2]. First satellites have shown the feasibility of the technology [3,4]. One of the next steps in satellite QKD development is to demonstrate QKD with a CubeSat mission. Several quantum communications CubeSat missions are currently in development, some for technology testing, some for implementation of a complete QKD system [5,6,7].

In both CubeSat based optical link use cases, telecommunication and quantum communications, similar challenges do exist. One of the biggest is the implementation of the required precise beam steering with a pointing, acquisition and tracking (PAT) system. The PAT system is often split into two subsystems, the coarse pointing assembly (CPA) and the fine pointing assembly (FPA). In CubeSat systems, the CPA can be implemented by the satellite busses body pointing (and tracking) capability. The FPA is often implemented with an active optical element within the optical system of the terminal.

This publication focuses on verification tests of the laser communication terminals (LCT) OSIRIS4CubeSat (O4C) and OSIRIS4QUBE (O4Q) for the CubeSats missions PIXL-1 and QUBE. PIXL-1 is a quasi-operational demonstrator mission for direct to Earth data downlinks. QUBE is an in-orbit mission to test and verify core components needed for a CubeSat QKD missions. In these tests, the verification of the PAT performance, i.e. the FPA, is in focus. Nevertheless, the transmission capabilities are tested and verified as well. Accordingly, the objective is to recreate the conditions that are anticipated in space through the implementation of a ground-to-ground test.

2. Terminal Design

O4C is the first LCT of DLR's optical space infrared downlink system (OSIRIS) family especially designed for CubeSats. The modular approach allows reuse of single subsystems and easy adaptions towards new and future applications. The laser beam divergence is 193 µrad (1/e² full angle). This precision requirement exceeds the abilities of common CubeSat attitude control systems (ACS). Thus, a high precision beam steering mechanism inside the LCT is required. Therefore, O4C is equipped with an FPA to correct the satellites residual pointing error up to ±1°.The functionality of the FPA is depicted in Fig. 1.

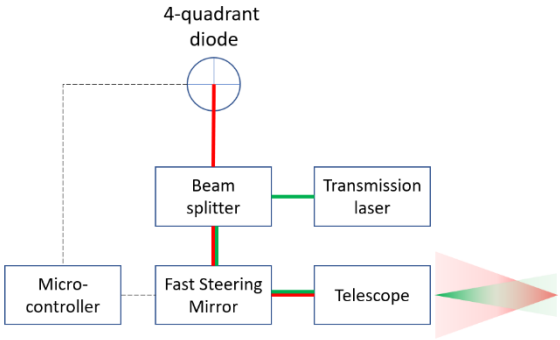

Fig. 1. Fine pointing assembly of OSIRIS4CubeSat and OSIRIS4QUBE

A beacon (red) with a wavelength of 1590 nm is sent by an optical ground station (OGS) and illuminates the satellite and the payload. The 4-quadrant diode (4-QD) measures the angular offset of the incoming beacon and provides feedback as a sensor input to the microcontroller. The microcontroller commands a fast steering mirror (FSM) to correct the measured error. The transmission beam (green) with 1550 nm wavelength shares the same optical path with the beacon. This guarantees that the transmission beam hits the OGS where the beacon is emitted and the transmission signal is received.

The goal of the project QUBE is to transmit low power pulses and polarization states in preparation of QKD on CubeSats. Two experimental quantum channels generated by payloads from Ludwig Maximilian University Munich (LMU) and Max Planck institute for the science of light (MPL) provide a quantum signal (850 nm LMU and 1571 nm MPL) while DLRs payload transmits a synchronization clock over a classical optical channel [5]. Therefore, the modular approach is used to adapt the O4C terminal to extend its capabilities towards QKD. The outcome is O4Q where the two quantum channels and the classical channel are coupled with a fiber network into the exact same optical path of O4Q. The modular approach of O4C allows to adapt single subsystems without having to completely redevelop the payload. In O4Q, most of the subsystems of O4C could be reused. Especially the FPA design could be reused which makes the operation concept identical. To extend O4C with the functionalities of QKD, mainly the optical system had to be changed.

The design and shape of the optomechanical system remains, with the exception of an elongation of the telescope length by 10 mm. The lens design is adapted to support wavelengths in the optical C- and L-band (DLR and MPL system) as well as 850 nm (LMU system). A combination of chalcogenide and heavy flint glasses are used to build achromatic doublets. Some of the lenses are aspherical to cope with aberrations for off-axis beams which occur in the telescope while the terminal is

tracking the ground beacon [8]. The complex optical system and the required compromise between divergence and tilt angle offset of the four different wavelengths lead to a different tracking and acquisition behaviour compared to O4C. To analyse the differences in the FPA behaviour between O4C and O4Q and to verify the link budget by measuring the data reception performance we tested both systems in an end-to-end test campaign before the launch.

3. Ground-to-ground test setup

For the development of LCTs, we follow the test-like-you-fly approach to prepare the developed payloads for space missions. All end-to-end tests are intended to be as close to the final mission conditions as possible. The goal of the two test campaigns for O4C and O4Q is to verify the functionalities of the LCTs. The first goal is to proof the tracking functionalities for both terminals even at low elevation links. The second goal is to demonstrate the successful data transmission and reception, also at low elevations. The purpose of the tests is the verification of the laser terminals themselves, only for the classical communication channel. The verification of the quantum channels in QUBE are not part of the campaigns described in this paper.

3.1 Setup

Fig. 2 shows a block diagram of the entire test setup, which is explained in detail below.

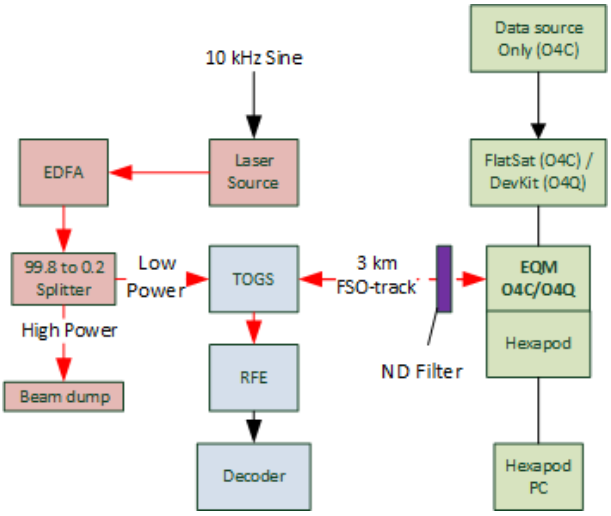

Fig. 2. Block diagram of the end-to-end test setup. Green parts are on transmitter side, blue is the optical ground station and red the beacon system for the PAT

On transmitter side (green), the engineering qualification model (EQM) is operated by a FlatSat (O4C) or a Devkit (O4Q). Both systems mimic the on-board computer and the required payloads during the final mission like e.g. the software defined radio. The hardware and the interfaces are identical to the flight hardware. A hexapod moves the EQMs in and around all three axes. This allows to replicate the satellites trajectory during a flyover.

For both campaigns DLR's transportable optical ground station (TOGS) was used on the receiver side (blue). It has a 60 cm Ritchey-Cassegrain telescope and is designed especially for technology demonstration and data reception. Behind the telescope is a receiver front end, a highly sensitive sensor that performs the optical-electrical conversion. An in-house developed modem collects the RFE signal and decodes the data sent by the EQM.

During the later PIXL-1 mission DLR's new OGS with an 80 cm mirror was used and will also be used during the QUBE mission. The beacon system of the TOGS and the new OGS are identical.

The beacon system (red) contains a 10 kHz sine signal generator which modulates the laser source to better distinguish it from background light at the receiver. The tap output of the internal splitter of the erbium doped fiber amplifier (EDFA) can be used as a low power signal while still operating it at full power. This is required as the signal form of the 10 kHz signal changes when the power is reduced. To replicate the mission conditions, all lasers have to be operated at full power. As a result, the signals must be attenuated optically (purple filter in Fig. 2).

3.2 Requirements and assumptions

During the ground-to-ground test, the transmitter is located in 3 km distance to the TOGS which marks the free-space track for the tests. To evaluate the setup for the campaign it is necessary to calculate the expected losses of the final missions, in comparison to the losses of the test scenario, in advance. The geometrical and the atmospheric losses are equal for up- and downlink and can therefore be calculated for both propagation ways.

The campaigns tested and verified the terminals for various scenarios like static and dynamic satellite behaviour or different elevation angles. The most important design driving mission requirement is link acquisition at 10° elevation for both terminals. Besides this minimum requirement scenario, a test for a 39.5° elevation link is additionally described exemplarily in this paper.

Both satellites fly in a sun-synchronous low Earth orbit. According to (1), the distance at 10° elevation in a 500 km example orbit is $d_{10} \approx 1695\ km$ and $d_{40} \approx 748\ km$ for a 39.5° elevation link, as derived with the following formula [9].

$$d = \frac{-2E\tan\alpha\sqrt{(2Etan(\alpha))^2 - 4(1+tan^2(\alpha))(E^2+T^2)}}{2(1+tax^2(\alpha))(\cos(\alpha))} \quad (1)$$

The geometrical power loss can be calculated using equation (2). Initially the power loss over 3 km distance

is $L_I \approx 207.7\,dB$. The losses for the simulated link distances are $L_{10} \approx 262.8\,dB$ for a 10° link and $L_{40} \approx 255.7\,dB$ for the 39.5° elevation link. This leads to a required additional attenuation of $a_{d10} = L_{10} - L_I = 55.1\,dB$ and $a_{d40} = L_{40} - L_I = 48\,dB$ compared to a 10° or 39.5° elevation satellite laser link.

$$L_{Ch} = \left(\frac{4\pi d}{\lambda}\right)^2 \triangleq 20\log_{10}\left(\frac{4\pi d}{\lambda}\right) dB \qquad (2)$$

Atmospheric losses, e.g. due to absorption, as well as scintillation effects also need to be considered. Atmospheric losses depend on a number of boundary conditions. Typical models lead to an attenuation of satellite-to-ground links with a total attenuation $a_{atm} = 4\,dB$ for low-elevation links (e.g. $T_Z = 0{,}92$ with elevation of about 5°, equation (16) in [10]). For simplicity, this number was used as a worst-case figure for all elevation angles.

Scintillation effects, however, can be constructive and destructive. They result in fluctuations around the mean power. Thus, scintillation effects are not considered in link budgets for laser communication systems and are not considered for scaling from the satellite- to ground-to-ground links [10].

This leads to a total attenuation of $a_{10} = a_{d10} + a_{atm} = 59.1\,dB$ for a 10° elevation link and $a_{40} = a_{d40} + a_{atm} = 52\,dB$ for a 39.5° elevation link. These are the expected optical losses in up- and downlink for the relevant in-orbit mission scenarios. The expected losses are summarized in the following Table 1.

Table 1. Expected power losses in up- and downlink channel during the final in-orbit missions for relevant scenarios

Elevation	**10°**	**39.5°**
	Expected losses [dB]	
Distance (diff.*)	55.1	48
Atmosphere (diff.*)	4	4
Total	**59.1**	**52**

* Difference between 3 km and mission distance

The optical signal of the transmission laser and the beacon laser have to be optically attenuated by the values described above. Both lasers have to run at full power as they will be operated during the final missions to keep signal integrity. A reduction of the output power is not useful as the modulation waveform changes for different power levels. Thus, it was decided to attenuate the signal with a neutral-density (ND) filter in the optical path (purple in Fig. 2). Uplink (reception, Rx) of the beacon and the downlink (transmission, Tx) were first tested separately and afterwards in a full end-to-end demonstration.

3.3 Uplink

The campaign started with the separated acquisition and tracking tests which uses only the uplink channel and can therefore be evaluated separately. The EDFAs that generate the uplink beacons at the TOGS have tap outputs, which makes it possible to operate them at their nominal power. At 4 W nominal mean output power, the tap output emits light with 7.84 mW measured. Two of these beacons will be used during the final mission to ensure transmitter diversity [11]. During the ground-to-ground test only one beacon can be used, because a second beacon would cause a parallaxes misinterpretation at the 4-QD of the EQM over this short distance. This loss of additional 3 dB compared to the mission has to be considered as well.

$$a_{EDFA} = 10\log_{10}\left(\frac{4\,W}{7.84\,mW}\right) dB + 3\,dB \approx 30.1\,dB \qquad (3)$$

To generate the losses which are expected in the final mission the ND filters attenuation must be at least $a_{ND10} = a_{10} - a_{EDFA} = 29\,dB$ and $a_{ND40} = a_{40} - a_{EDFA} = 21.9\,dB$. Atmospheric losses and scintillation over the 3 km ground-to-ground track are not considered to follow the worst-case scenario approach. Commercially available ND filters do not exactly match the attenuations described above which leads to the setup summarized in Table 2.

Table 2. Attenuation for separated uplink (Rx) tests of the relevant mission scenarios

Elevation	**10°**	**39.5°**
	Replicated attenuation [dB]	
EDFA*	30.1	30.1
ND filter	30.1	22.7
Total	**60.2**	**52.8**

* Difference to maximum output power

It can be seen that the setup used in the campaign replicates the mission conditions for the isolated uplink tests as the attenuations in Table 2 overcomes the expected losses in Table 1.

3.4 Downlink

With a divergence of 193 µrad (1/e², full diameter), the diameter at which the optical power dropped to 1/e² after 3 km free space distance is 579 mm. The TOGS telescope has a diameter of 600 mm primary mirror and an obscuration of 160 mm. Since the beacon collimators are mounted on platforms located next to the mirror, the center of the beacon is 320 mm offset from the center of the TOGS telescope (black dot in Fig. **3**). Tracking on one of the two beacons will therefore induce additional loss to the link over 3 km, since part of the transmission

laser of the EQM is cut off. This is visualized in Fig. 3 where the overlap of the receive aperture and the beam footprint are depicted.

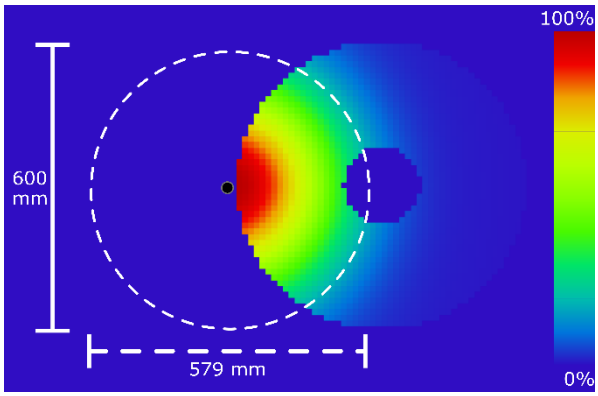

Fig. 3. Beam shape incident onto TOGS telescope, with the beam footprint is depicted by the dashed circle

The intensity profile of the transmission beam is color coded with maximum intensity in red. Only the section of the beam is shown which is coupled into the TOGS telescope and the transmission beam is indicated by a dashed white circle which represents the $1/e^2$ diameter. The additional loss for the link is 5 dB which also includes the obscuration from the secondary mirror of the TOGS (M2). This is important for the interpretation of the transmission tests of the classical channel, but not for the tracking. The evaluated 5 dB have to be reduced for the ND filter for these tests to recreate realistic conditions.

3.5 End-to-end setup

The full end-to-end test involved the test of the data transmission in the downlink including the tracking effects of the terminal. Thus, the setup has to replicate the conditions for up- and downlink at the same time to rebuild realistic conditions comparable to the in-orbit mission.

The setup described in subchapter 3.3 has to be adapted as the attenuation matches the conditions of the uplink channel but not the expected losses in the downlink. The transmitter of the EQM has to run at full power and does not contain a tap output like the EDFA at the TOGS. Thus, the Tx-signal has to be additionally attenuated by 30.1 dB. As this attenuation is realized by the ND filter, it comes with the disadvantage that it attenuates the beacon signal as well. Hence, the EDFA has to use the high-power output instead. For these tests still only one EDFA can be used due to parallaxes errors which changes the power reductions replicated by the EDFA from 30.1 dB to 3 dB in the uplink.

The descriptions in the previous sections lead to the attenuation setups in Table 3 during the full end-to-end tests of up- and downlink running in parallel.

Table 3. Attenuation during the end-to-end test including up- (Rx) and downlink (Tx) tests of the relevant mission scenarios

Elevation	**10°**	**39.5°**
	Replicated attenuation [dB]	
EDFA* (only Rx)	3	3
ND filter	57.2	50.4
Coupling (only Tx)	5	5
Total (Rx)	**60.2**	**53.4**
Total (Tx)	**62.2**	**55.4**

* Difference to maximum output power

The ND filter effects both up- and downlink equally. The attenuation caused by the EDFA only effects the uplink (Rx) and the coupling losses only effect the downlink (Tx). It is intended that a full end-to-end test is performed to analyse the downlink data transmission while the terminal is tracking on the uplink beacon signal. Thus, the total attenuation of the setup has to overcome the expected losses described in Table 1 in both channels. Table 3 shows that the commercially available ND filters where selected so that the resulting setup overcomes the requirements of the relevant scenario (Table 1) in up- and downlink channel. This leads to a headroom of more than 1 dB in the uplink (Rx) and more than 3 dB in the downlink (Tx) path.

4. Results

Comparable tests were carried out for O4C and O4Q. The aim of these tests is to validate the functionality of the full end-to-end chain and to check the performance under changing environmental conditions.

4.1 Acquisition and tracking (uplink)

The acquisition and tracking results are illustrated by the tilting of the mirror. Fig. 4, Fig. 5 and Fig. 6 show the mirror's deflection in x- (blue) and y-axis (orange) over time. The angles of the mirror are represented as the integer values of the digital analogue converter (DAC) where $+2^{16}/2$ stands for the maximum beam deflection of +1° and $-2^{16}/2$ for -1° (all angles ex-aperture). The value 0 stands for the center position of the mirror. The triangles in the diagrams show the search spiral during the pointing phase. Straight lines represent a static mirror while the terminal is tracking on the beacon. Deviations from this straight line result because of corrections by the mirror due to the simulated satellites movement, caused by the hexapod.

The static acquisition was evaluated first in the campaigns (see Fig. 4). This represents the ideal scenario and allows conclusions to be drawn about the absolute minimum tracking performance. Another test consists of first deflecting the Hexapod in 0.1° steps in one axis in both directions and then repeating the same with the other axis. This ensures that tracking is possible over the entire

field of regard (FoR), in the case of O4C and O4Q that equals ±1°. When switching to the dynamic scenario, a random trajectory is executed by the hexapod. It moves within the FoR, whereby the direction can be adjusted every second. The maximum error drift speed was set to the worst-case value of 0.08°/s, a specification that comes from the satellite manufacturer for the satellites CubeL in the PIXL-1 mission and QUBE.

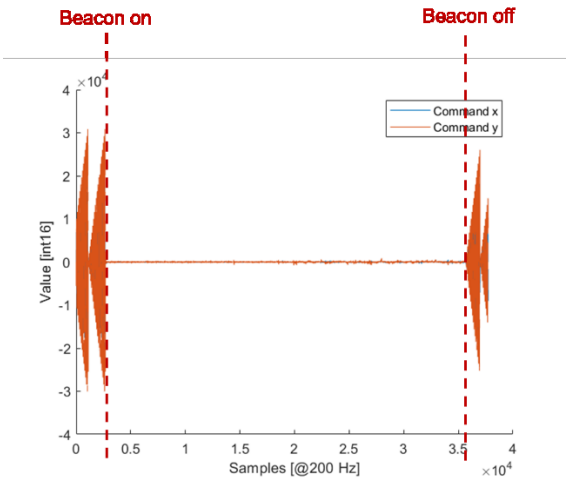

Fig. 4. Initial static test of O4C to demonstrate successful acquisition and tracking at 39.5°

The test procedure will be described with respect to Fig. 4 using the end-to-end campaign test data from O4C. First, the LCT under test is initialized so that the configuration for the following link is transferred to the microcontroller. The downlink process is then started. It performs an internal offset calibration in order to subtract the background light from the signal processing chain. Once this process has been completed, the spiral is started so that the terminal is ready for acquisition. Only then is the beacon on the ground station side activated. As soon as this is detected on the 4-QD, the system switches to tracking mode. Tracking is maintained until the signal on the 4-QD disappears again. In this case by switching off the beacon. In the direct-to-earth scenario, this can be equated to a cloud or falling below the required elevation.

In Fig. 5, the hexapod is now used to move the trajectory in addition to the static acquisition. It can be seen that the LCT is able to track over the entire test period. The values of the four quadrants of the 4-QD largely maintain their level, so that a low control error can be concluded.

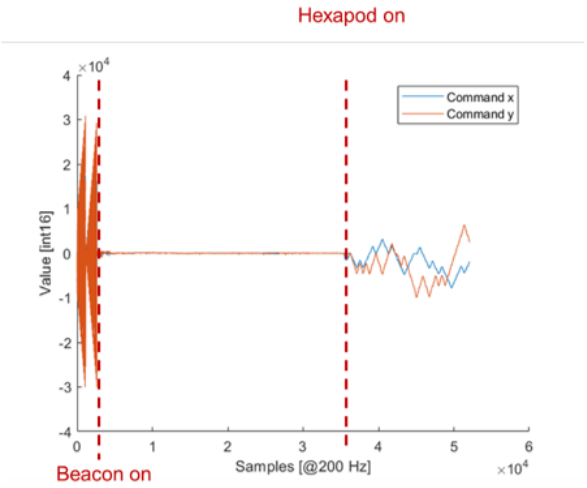

Fig. 5. O4C in a dynamic scenario using the hexapod to emulate the satellites error trajectory at 39.5°

In Fig. 6 the same dynamic scenario is shown. However, an attenuation which corresponds to 10° of elevation is used to determine the behaviour at long distances through the atmosphere, which yields more remaining jitter than before. O4C is still able to perform closed-loop tracking and a reacquisition within one spiral period after the loss of signal. During the dynamic scenario, the terminal was able to track the beacon 97% of the time with a tracking consistency of 99%. Even when the signal was lost, the terminal was able to reobtain tracking within 50 ms, 99% of the time.

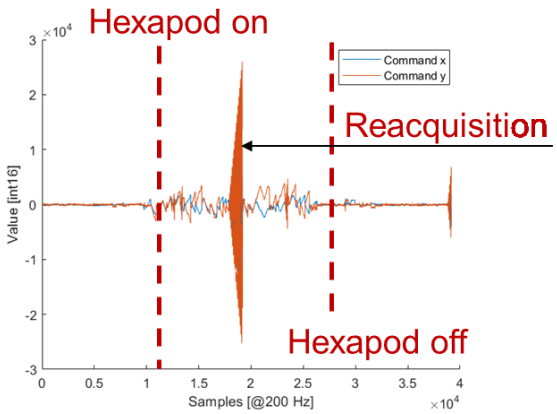

Fig. 6. O4C in the highly attenuated scenario of 10° of elevation

Acquisition and tracking were demonstrated in the static and dynamic cases. However, it is also important to ensure that the entire FoR is covered. The special feature of O4Q is that it has the same possibilities as O4C with regard to the FoR. However, the more complex optics are optimized for a range of only ±0.6° while O4C is designed for a FoR of ±1°. Therefore, anything outside this range is desirable but not absolutely necessary for the

success of the mission. Thus, the test with O4Q can be seen in Fig. **7** as it has higher limitations of the FoR than O4C. In contrast to the previous figures, Fig. 7 shows again the integer values of the mirror`s DAC output, but with separated plots for x- and y-axis where 0 stands for -1°, $2^{16}/2$ stands for the center position and 2^{16} for the maximum deflection of +1° of the mirror. Additionally, Fig. 7 shows the received power on the 4-QD also as integer values of the analogue digital converter output. In the experiment, it can be noticed that the x-axis first travels through the entire positive range and then, after returning to the centre, travels through the entire negative range. The experiment is then repeated with the y-axis. Here, it can be seen that there is an instability at 0.7°. However, re-acquisition is successful so that the rest of the range can be traversed. In the negative direction, a short re-acquisition is carried out at -0.6°. But here too, the entire range can then be traversed and tracked successfully.

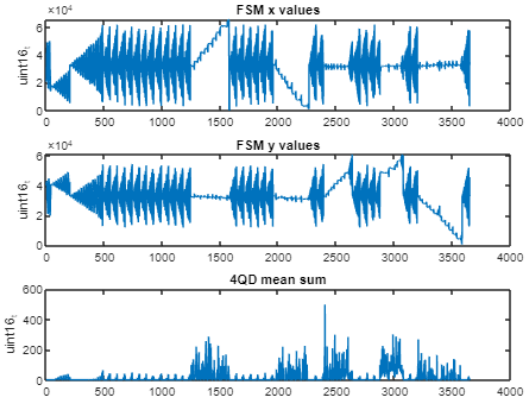

Fig. 7. The experiment with O4Q shows that tracking in both axis over the full range is possible

4.2 Data transmission (downlink)

In O4C, the data transmitted from the terminal during the tests were processed to overcome the atmospheric effects of the free space optical channel [12]. After fragmenting, encoding, interleaving and scrambling, synchronization markers are attached to the outgoing data frames. At the receiver side, an in-house developed RFE was used to perform the optical-electrical conversion of the incoming optical signal. The output digital signal was then fed into the in-house developed modem which oversamples the incoming data stream to recover the data (O4C) or the clock (O4Q). For O4C, the data is further analysed to look for synchronization markers attached at the transmit side. Once a few of such markers are detected, the modem is considered to be synchronized and the data received thereafter is collected.

During these tests, a single processed picture was transmitted in an infinite loop. In the 39.5° elevation link tests, all transmitted pictures could successfully be decoded without any errors. Further tests where performed and showed that error-free pictures could be re-assembled up to a total attenuation of 59.3 dB. For the 10° elevation post processing was required. Nevertheless, a transmission at 62.2 dB attenuation was still possible, but with a higher packet loss. Hence, the modem provides configuration for the re-assembler to extract a single picture by assembling best frames collected during different parts of the transmission. This proved the end-to-end transmission including en- and decoding even for lowest elevations.

O4Q sends a clock instead of data over the classical optical channel. At the time of the campaign the final receiver provided by LMU and MPL were not available, to demonstrate the full end-to-end chain. Thus, the amplitude of the received analogue signal was measured and compared with the signal from O4C. It turned out that the amplitude of the clock signal of O4Q is higher than the amplitude of the signal measured during the O4C campaign. This was expected as the clock has a frequency of 10 MHz while O4C transmits 100 Mbit/s on-off-keying which is comparable to 50 MHz. The longer positive half-wave of the clock signal explains the higher amplitude due to the longer time of photon collection at the RFE.

5. Discussion

Both terminals were examined on the same test track. The analysis of the recorded telemetry shows that both are able to guarantee both acquisition and tracking in all cases examined. Both the minimum and maximum distances occurring in low earth orbit were analysed. It is pleasing to note that O4Q is also able to establish links over the entire FoR. Beside the tracking behaviour, it could be shown that a successful data transmission is possible as well. The results make the base for the missions PIXL-1 (O4C) and QUBE (O4Q) and prove the flight readiness of both systems.

The assumptions made during the ground-to-ground tests were always conservative, to give the link budget a reasonable margin, which defines the worst-case approach followed during both campaigns. The setup still gives room for improvement as the OGS which will be used in the final mission has a larger aperture of 80 cm. Furthermore, experiments with other LCTs show that the beacon divergence can be reduced from 1 $mrad$ to 0.5 $mrad$ and hence quadruple the optical uplink power density if required.

During the PIXL-1 mission several downlinks were successfully performed with O4C. Whenever the satellite CubeL was pointing correctly to the OGS, an optical connection could be established. This behaviour is reproducible whenever the required preconditions are

given. The telemetry shows afterwards that the received optical power inside the system overcomes the expectations from the link budget and the results of the ground-to-ground test described in this paper. Successful link acquisition, stable tracking and error-free data transmission are possible even below 10° elevation, even though O4C operates with only 60% of its maximum optical power.

6. Conclusion

This paper shows that a ground-to-ground test can rebuild in-orbit scenarios for classical laser communication and quantum key distribution on CubeSats. It is possible to simulate the behaviour of the satellite and to recreate the conditions of a space mission. The comparison with the results of the PIXL-1 mission show that the worst-case approach was successful to have a reasonable headroom in the link budget.

Since the results of O4C have already been verified by direct-to-earth downlinks in the low earth orbit, it can be concluded that O4Q will show the desired performance in the QUBE mission as well. QUBE started on August 16th 2024 with the Transporter 11 mission and is currently in the commissioning phase.

Acknowledgements

This research was partly conducted within the scope of the project QUBE and QUBE II, funded by the German Federal Ministry of Education and Research (BMBF) under the funding codes 16KIS0767 and 16KISQ051. The authors give special thanks to the colleagues of Tesat Spacecom, Ludwig-Maximilians University Munich, Max-Planck Institute for the Science of Light, Center for Telematics, and OHB Systems, who worked together in this experiment.

References

[1] Patricia Martín Pimentel, Benjamin Rödiger et al., Cube laser communication terminal (CubeLCT) state of the art, Acta Astronautica, volume 211, 2023, pages 326-332, ISSN 0094-5765, https://doi.org/10.1016/j.actaastro.2023.06.026.

[2] N. Gisin et al., Quantum cryptography, Rev. Mod. Phys. volume 74, 2002, pages 145–195

[3] S.-K. Liao et al., Satellite-to-ground quantum key distribution, Nature 549(7670), Springer Nature (2017), 43–47

[4] S.-K. Liao et al., Space-to-Ground Quantum Key Distribution Using a Small-Sized Payload on Tiangong-2 Space Lab, Chinese Physics Letters 34(9), 90302, IOP Publishing (2017)

[5] L. Knips et al., QUBE – Towards Quantum Key Distribution with Small Satellites, in Quantum 2.0 Conference and Exhibition, Optica Publishing Group (2022)

[6] M. Hutterer et al., QUBE-II – Quantum Key Distribution with a CubeSat, in Prof. of IAC 2022

[7] D. C. Craig. et al., Responsive Operations for Key Services (ROKS): A Modular, Low SWaP Quantum Communications Payload., 2022.

[8] C. Menninger, F. Moll, B. Rödiger, Dual wavelength optical system for multiple quantum communication transmitters in Cubesat platform, Proc. SPIE 11852, International Conference on Space Optics — ICSO 2020, 118525M (11 June 2021); https://doi.org/10.1117/12.2599965

[9] C., Ryu, HG. Compensation System Design and Comparison of Very High Doppler Frequency Effect. Wireless Pers Commun 108, 879–894 (2019). https://doi.org/10.1007/s11277-019-06436-5

[10] D. Giggenbach, M. T. Knopp, C. Fuchs, Link budget calculation in optical LEO satellite downlinks with on/off-keying and large signal divergence: A simplified methodology, International Journal of Satellite Communications and Networking, 41 (5), pages 460-476. Wiley. doi: 10.1002/sat.1478. ISSN 1542-0973.

[11] Kim, Isaac I. et. al, Scintillation reduction using multiple transmitters, Free-Space Laser Communication Technologies IX, 1997, Vol. 2990, p. 102-113

[12] https://public.ccsds.org/Pubs/142x0b1.pdf, Blue Book, OPTICAL COMMUNICATIONS CODING AND SYNCHRONIZATION, RECOMMENDED STANDARD CCSDS 142.0-B-1